

Extraction of P_{11} resonances from πN data

H. Kamano,¹ S. X. Nakamura,¹ T.-S. H. Lee,^{1,2} and T. Sato^{3,1}

¹*Excited Baryon Analysis Center (EBAC),
Thomas Jefferson National Accelerator Facility,
Newport News, Virginia 23606, USA*

²*Physics Division, Argonne National Laboratory, Argonne, Illinois 60439, USA*

³*Department of Physics, Osaka University, Toyonaka, Osaka 560-0043, Japan*

Abstract

We show that two P_{11} nucleon resonance poles near the $\pi\Delta$ threshold, obtained in several analyses, are stable against large variations of parameters within a dynamical coupled-channels analysis based on meson-exchange mechanisms. By also performing an analysis based on a model with a bare nucleon state, we find that this two-pole structure is insensitive to the analytic structure of the amplitude in the region below πN threshold. Our results are $M_{\text{pole}} = (1363_{-6}^{+9} - i 79_{-5}^{+3})$ MeV and $(1373_{-10}^{+12} - i 114_{-9}^{+14})$ MeV. We also demonstrate that the number of poles in the $1.5 \text{ GeV} \leq W \leq 2 \text{ GeV}$ region could be more than one, depending on how the structure of the single-energy solution of SAID is fitted. For three-pole solutions, our best estimated result of a pole near $N(1710)$ listed by Particle Data Group is $(1829_{-65}^{+131} - i 192_{-110}^{+88})$ MeV which is close to the results of several previous analyses. Our results indicate the need of more accurate πN reaction data in the $W > 1.6 \text{ GeV}$ region for high precision resonance extractions.

PACS numbers: 14.20.Gk, 13.75.Gx, 13.60.Le

I. INTRODUCTION

An important task in hadron physics is to extract nucleon resonances from πN reaction data. The extracted resonance parameters are needed to understand the spectrum and structure of excited nucleons within QCD. They are also the starting point for analyzing electromagnetic meson production reaction data which have been of high precision and extensive in recent years [1].

There exists several approaches [2–14] to extract nucleon resonances (N^*) from πN reaction data. In general, almost all 4-stars nucleon resonances listed by Particle Data Group [15] (PDG) are found in all approaches. However the existence of some N^* states, in particular those in the higher mass region, is controversial. The most investigated case is the number of resonances in πN P_{11} partial wave. In the region near Roper $N(1440)$, two poles close to the $\pi\Delta$ threshold were found in Refs. [3–5, 12] and in our recent extraction [14], while only one pole in the similar energy region was reported in Refs. [6, 9, 10]. In the higher mass region, the $N(1710)$ in P_{11} πN partial-wave is not reported in Refs. [5, 12], but is identified in all other analysis [2, 3, 6–11, 14].

To make progress, it is important to address a commonly asked question on the extent to which the extracted resonance parameters depend on the reaction models employed and the accuracy of the empirical partial-wave amplitudes used in the analysis. For P_{11} resonances, this was investigated by Cutkosky and Wang [3] and more recently by Ceci, Svarc, and Zauner [9] within the Carnegie-Mellon University-Berkeley model [2] (CMB). In an analysis including πN , ηN and pseudo $\pi\pi N$ channels, it was demonstrated [9] that the existence of $N(1710)$ depends on the structure of the πN amplitude which is related to the coupled-channels effects due to ηN channel. In this work, we carry out a similar investigation within a dynamical coupled-channels model [16] (EBAC-DCC). The main difference between our approach and CMB model is to define the non-resonant amplitude by using the meson-exchange mechanisms. We thus have provided additional information for examining the dependence of the P_{11} resonances on the reaction models employed in the analysis.

Our investigation has two parts. First we would like to examine the stability of the two-pole structure of P_{11} resonances near the $\pi\Delta$ threshold ($W \sim 1.3$ GeV). Our objective is to examine how this two-pole structure is sensitive to the parameters of the meson-exchange mechanisms within the EBAC-DCC model used in our extraction [14]. In the fits [17] (JLMS) of πN data [5], these parameters were determined within the ranges known from previous studies of meson-exchange mechanisms. Here we allow them to vary much more freely such that several models with different analytic properties are obtained for examining whether the resulting pole positions are stable within the EBAC-DCC model.

The two-pole structure is also reported by Döring *et al.* [12] in an analysis based on a meson-exchange model with a bare nucleon state [18]. As discussed in Ref. [19], the analytic structure of this model as well as other similar models [20–22] is rather different from the EBAC-DCC model, in particular in the region near the nucleon pole, mainly because of the differences in deriving [23] three-dimensional scattering equations from relativistic quantum field theory. To further examine the stability of the two-pole structure of P_{11} resonances and the existence of $N(1710)$ state within the meson-exchange models, we also perform fits by using such a model. Our formulation is similar to that developed by Pearce and Afnan [20].

We will show that the positions of two poles near the $\pi\Delta$ threshold extracted from all of the meson-exchange models constructed here are rather stable. This explains why the similar two-pole structure is also found in the other analyses [3, 5, 12] which use very different

reaction models.

The second part of our investigation is to examine the extent to which the structure of the P_{11} amplitude in higher invariant mass (W) region can influence the two-pole structure near the $\pi\Delta$ threshold. Here we also follow Ref. [9] to examine how the number of resonance states in the region near $N(1710)$ state listed by PDG depend on the structure of the data. We thus consider both the energy-dependent and single-energy solutions (SP06) of SAID [5], hereafter we call them SAID-EDS and SAID-SES, respectively, as well as a solution from CMB [3] collaboration. The CMB amplitudes could be outdated, but is used here only for investigating the dependence of the P_{11} poles on the accuracy of the data. We will show that the number of resonance poles in the $1.6 \text{ GeV} < W < 2 \text{ GeV}$ could be more than one, depending on how the structure of the amplitude is fitted. Our results indicate the importance of improving the accuracy of empirical partial-wave amplitudes. More accurate πN reaction data from the new hadron facilities, such as the Japan Proton Accelerator Research Complex (J-PARC), are needed. Our conclusion is consistent with the finding of Ref. [9] in which the importance of also fitting the $\pi N \rightarrow \eta N$ amplitude is demonstrated in identifying P_{11} $N(1710)$ state.

In Sec. II, we give a brief description of the coupled-channels models used in this work. The results are given and discussed in Sec. III. Section IV is devoted to the discussions on possible further developments.

II. DYNAMICAL COUPLED-CHANNELS MODELS

In this section we first recall briefly the EBAC-DCC model [16] used in this work. We then describe how the model can be modified to obtain a model with a bare nucleon, which has the main feature of other πN reaction models with a bare nucleon [12, 20–22].

A. EBAC-DCC model

The EBAC-DCC model describes meson-baryon reactions involving the following channels: πN , ηN , and $\pi\pi N$ which has $\pi\Delta$, ρN , and σN resonant components. The excitation of the internal structure of a baryon (B) by a meson (M) to a bare N^* state is modeled by a vertex interaction $\Gamma_{MB\leftrightarrow N^*}$. The meson-baryon (MB) states can interact via interactions $v_{MB,M'B'}$ which describe the meson-exchange mechanisms deduced from phenomenological Lagrangians. Within the model, the partial-wave amplitude of the $M(\vec{k}) + B(-\vec{k}) \rightarrow M'(\vec{k}') + B'(-\vec{k}')$ reaction can be cast into the following form (suppressing the angular momentum and isospin indices):

$$T_{MB,M'B'}(k, k', E) = t_{MB,M'B'}(k, k', E) + t_{MB,M'B'}^R(k, k', E), \quad (1)$$

where the first term is defined by a set of coupled-channels integral equations

$$t_{MB,M'B'}(k, k', E) = v_{MB,M'B'}(k, k') + \sum_{M''B''} \int_{C_{M''B''}} q^2 dq v_{MB,M''B''}(k, q) G_{M''B''}(q, E) t_{M''B'',M'B'}(q, k', E). \quad (2)$$

Here C_{MB} is the integration contour in the complex- q plane used for the channel MB . The term associated with the bare N^* states in Eq. (1) is

$$t_{MB,M'B'}^R(k, k', E) = \sum_{i,j} \bar{\Gamma}_{MB \rightarrow N_i^*}(k, E) [D(E)]_{i,j} \bar{\Gamma}_{N_j^* \rightarrow M'B'}(k', E), \quad (3)$$

where the dressed vertex function $\bar{\Gamma}_{N_j^* \rightarrow M'B'}(k, E)$ is calculated [17] from the bare vertex $\Gamma_{N_j^* \rightarrow M'B'}(k)$ and convolutions over the amplitudes $t_{MB,M'B'}(k, k', E)$. The inverse of the propagator of dressed N^* states in Eq. (3) is

$$[D^{-1}(E)]_{i,j} = (E - m_{N_i^*}^0) \delta_{i,j} - \Sigma_{i,j}(E), \quad (4)$$

where $m_{N_i^*}^0$ is the bare mass of the i -th N^* state, and the N^* self-energy is defined by

$$\Sigma_{i,j}(E) = \sum_{MB} \int_{C_{MB}} q^2 dq \bar{\Gamma}_{N_j^* \rightarrow MB}(q, E) G_{MB}(q, E) \Gamma_{MB \rightarrow N_i^*}(q, E). \quad (5)$$

Defining $E_\alpha(k) = [m_\alpha^2 + k^2]^{1/2}$ with m_α being the mass of particle α , the meson-baryon propagators in the above equations are: $G_{MB}(k, E) = 1/[E - E_M(k) - E_B(k) + i\epsilon]$ for the stable πN and ηN channels, and $G_{MB}(k, E) = 1/[E - E_M(k) - E_B(k) - \Sigma_{MB}(k, E)]$ for the unstable $\pi\Delta$, ρN , and σN channels. The self energy $\Sigma_{MB}(k, E)$ is calculated from a vertex function defining the decay of the considered unstable particle in the presence of a spectator π or N with momentum k . For example, we have for the $\pi\Delta$ state,

$$\Sigma_{\pi\Delta}(k, E) = \frac{m_\Delta}{E_\Delta(k)} \int_{C_3} q^2 dq \frac{M_{\pi N}(q)}{[M_{\pi N}^2(q) + k^2]^{1/2}} \frac{|f_{\Delta \rightarrow \pi N}(q)|^2}{E - E_\pi(k) - [M_{\pi N}^2(q) + k^2]^{1/2} + i\epsilon}, \quad (6)$$

where $M_{\pi N}(q) = E_\pi(q) + E_N(q)$ and $f_{\Delta \rightarrow \pi N}(q)$ defines the decay of the $\Delta \rightarrow \pi N$ in the rest frame of Δ , C_3 is the corresponding integration contour in the complex- q plane. The self-energies for the ρN and σN channels are similar.

To search for resonance poles, the contours C_{MB} and C_3 must be chosen appropriately to solve Eqs. (2)-(6) for E on the various possible sheets of the Riemann surface. The procedures for performing this numerical task have been discussed in Ref. [14, 24]. Like all previous works [5, 10], we only look for poles which are close to the physical region and have effects on the πN scattering observables. All of these poles are on the unphysical sheet of the πN channel, but could be on either unphysical (u) or physical (p) sheets of other channels considered in this analysis. We will indicate the sheets where the identified poles are located by $(s_{\pi N}, s_{\eta N}, s_{\pi\pi N}, s_{\pi\Delta}, s_{\rho N}, s_{\sigma N})$, where s_{MB} and $s_{\pi\pi N}$ can be u or p .

B. Model with a bare nucleon state

To examine further the model dependence of resonance extractions, it is useful to also perform analysis using models with a bare nucleon, as developed in, for example, Refs. [12, 20–22]. Within the formulation given in Sec. II A, such a model can be obtained by adding a bare nucleon (N_0) state with mass $m_{N_0}^0$ and $N_0 \rightarrow MB$ vertices and removing the direct $MB \rightarrow N \rightarrow M'B'$ in the meson-baryon interactions $v_{MB,M'B'}$. All numerical procedures for this model are identical to that used in the JLMS analysis, except that the resulting

amplitude must satisfy the nucleon pole condition. Here we follow the procedure of Afnan and Pearce [20].

For simplicity, we include one bare N_0 state and only one bare N^* state. The amplitude can still be written in the form of Eq. (1) and the propagator $D(E)$ of the term t^R of Eq. (3) is a 2×2 matrix. The nucleon pole condition can be most transparently defined by introducing an orthogonal matrix $U^T U = 1$ ($U_{ij}^T = U_{ji}$) to diagonalize $D^{-1}(E)$ of Eq. (4). The term $t_{\pi N, \pi N}^R$ of Eq. (3) can then be cast into the following diagonal form

$$t_{\pi N, \pi N}^R(k, k, E) = \sum_{i=1,2} \tilde{t}_{\pi N, \pi N}^i(k, k, E), \quad (7)$$

with

$$\tilde{t}_{\pi N, \pi N}^i(k, k, E) = \frac{\tilde{F}_{\pi N, i}(k) \tilde{F}_{i, \pi N}(k)}{E - m_i^0 - \tilde{\Sigma}_i(E)}, \quad (8)$$

where $m_1^0 = m_N^0$ and $m_2^0 = m_{N^*}^0$, and the mass shifts are

$$\begin{aligned} \tilde{\Sigma}_1(E) &= \frac{1}{2} \{ m_2^0 - m_1^0 + \Sigma_{11}(E) + \Sigma_{22}(E) \\ &\quad - [(m_2^0 + \Sigma_{22}(E) - m_1^0 - \Sigma_{11}(E))^2 + 4\Sigma_{12}^2(E)]^{1/2} \}, \end{aligned} \quad (9)$$

$$\begin{aligned} \tilde{\Sigma}_2(E) &= \frac{1}{2} \{ m_1^0 - m_2^0 + \Sigma_{11}(E) + \Sigma_{22}(E) \\ &\quad + [(m_2^0 + \Sigma_{22}(E) - m_1^0 - \Sigma_{11}(E))^2 + 4\Sigma_{12}^2(E)]^{1/2} \}. \end{aligned} \quad (10)$$

Here $\Sigma_{i,j}(E)$ are defined by Eq. (5). The transformed vertices in Eq. (8) are

$$\tilde{F}_{i, \pi N}(k) = \sum_j U_{i,j} \bar{\Gamma}_{N_j^* \rightarrow \pi N}(k), \quad (11)$$

$$\tilde{F}_{\pi N, i}(k) = \sum_j U_{i,j} \bar{\Gamma}_{\pi N \rightarrow N_j^*}(k), \quad (12)$$

where $N_j^* = N_0$ or N^* , and the transformation operator U is defined by

$$U_{11} = U_{22} = \frac{1}{(1 + \nu^2)^{1/2}}, \quad (13)$$

$$U_{12} = -U_{21} = \frac{\nu}{(1 + \nu^2)^{1/2}}, \quad (14)$$

with

$$\nu = \frac{\Sigma_{11} - \tilde{\Sigma}_1}{\Sigma_{12}} = -\frac{\Sigma_{22} - \tilde{\Sigma}_2}{\Sigma_{12}}. \quad (15)$$

Suppose $E = m_N$ pole is found in the first term of Eq. (7), we then expand

$$\begin{aligned} E - m_1^0 - \tilde{\Sigma}_1(E) &= E - m_1^0 - \left\{ \tilde{\Sigma}_1(m_N) + \left[\frac{\partial}{\partial E} \tilde{\Sigma}_1(E) \right]_{E=m_N} (E - m_N) + \dots \right\} \\ &= (E - m_N) \left\{ 1 - \left[\frac{\partial}{\partial E} \tilde{\Sigma}_1(E) \right]_{E=m_N} + \dots \right\}, \end{aligned} \quad (16)$$

where we have defined the nucleon pole

$$m_N = m_1^0 + \tilde{\Sigma}_1(m_N). \quad (17)$$

This is the first nucleon pole condition taken into account in constructing the bare nucleon model.

Defining the renormalized vertex as

$$\begin{aligned} F_{\pi NN}(k) &= \tilde{F}_{1,\pi N}(k) Z^{-1/2} \\ &= \sum_j U_{1,j} \bar{\Gamma}_{j,\pi N}(k) Z^{-1/2}, \end{aligned} \quad (18)$$

with

$$Z = 1 - \left[\frac{\partial}{\partial E} \tilde{\Sigma}_1(E) \right]_{E=m_N}, \quad (19)$$

we then have

$$\tilde{t}_i^R(k \rightarrow k_{\text{on}}, k \rightarrow k_{\text{on}}, E \rightarrow m_N) = -\frac{[F_{\pi NN}(k_{\text{on}})]^2}{E - m_N}. \quad (20)$$

Here the on-shell momentum is defined by $E = \sqrt{m_N^2 + k_{\text{on}}^2} + \sqrt{m_\pi^2 + k_{\text{on}}^2}$. Below $E = m_N + m_\pi$, k_{on} becomes positive or negative imaginary. Here we take the positive imaginary since we look for the physical nucleon pole. The second nucleon pole condition then defines the renormalized vertex $F_{\pi NN}(k_{\text{on}})$ as the physical πNN form factor. Following the partial-wave decomposition procedure given in Ref. [16], we find

$$F_{\pi NN}(k_{\text{on}}) = F_{\pi NN}^{\text{phys.}}(k_{\text{on}}), \quad (21)$$

with

$$F_{\pi NN}^{\text{phys.}}(k) = -\frac{i}{(2\pi)^{3/2}} \frac{f_{\pi NN}}{m_\pi} \sqrt{12\pi k} \sqrt{\frac{E_N(k) + m_N}{2E_N(k)}} \frac{1}{\sqrt{2\omega_\pi(k)}} \left[1 + \frac{E_\pi(k)}{E_N(k) + m_N} \right], \quad (22)$$

where $f_{\pi NN} = \sqrt{4\pi \times 0.08}$. Following the previous approach, the bare $N_0 \rightarrow \pi N$ vertex $\Gamma_{N_0,\pi N}(k)$ is parameterized as Eq. (22) except that $f_{\pi NN}$ is replaced by a bare coupling constant $f_{\pi NN}^0$, and the form factor is introduced. Explicitly, it is written as

$$\Gamma_{N_0,\pi N}(k) = -\frac{i}{(2\pi)^{3/2}} \frac{f_{\pi NN}^0}{m_\pi} \sqrt{12\pi k} \sqrt{\frac{E_N(k) + m_N}{2E_N(k)}} \frac{1}{\sqrt{2\omega_\pi(k)}} \left[1 + \frac{E_\pi(k)}{E_N(k) + m_N} \right] F(k, \Lambda_{\pi NN}), \quad (23)$$

where we use the following form factor,

$$F(k, \Lambda_{\pi NN}) = \left(\frac{\Lambda_{\pi NN}^2}{k^2 + \Lambda_{\pi NN}^2} \right)^2. \quad (24)$$

The cutoff parameter $\Lambda_{\pi NN}$ of the form factor and the bare coupling constant $f_{\pi NN}^0$ are varied along with other parameters of the model to fit the empirical πN scattering amplitudes and the pole conditions (17) and (21).

TABLE I: The resonance pole positions M_R for P_{11} [listed as $(\text{Re}M_R, -\text{Im}M_R)$ in the unit of MeV] extracted from various parameter sets. The location of the pole is specified by, e.g., $(s_{\pi N}, s_{\eta N}, s_{\pi\pi N}, s_{\pi\Delta}, s_{\rho N}, s_{\sigma N}) = (upuupp)$, where p and u denote the physical and unphysical sheets for a given reaction channel, respectively. χ_{pd}^2 is defined by Eq. (26).

Model	$upuupp$	$upuppp$	$uuuuup$	$uuuuup$	χ_{pd}^2
SAID-EDS	(1359, 81)	(1388, 83)	—	—	2.94
JLMS	(1357, 76)	(1364, 105)	—	(1820, 248)	3.55
$1N^*$ -3p-H	(1357, 74)	(1363, 111)	—	(1792, 280)	2.41
$1N^*$ -3p-L	(1359, 69)	(1371, 112)	—	(1940, 242)	5.33
$2N^*$ -3p	(1368, 82)	(1375, 110)	—	(1810, 82)	3.28
$2N^*$ -4p	(1372, 80)	(1385, 114)	(1636, 67)	(1960, 215)	3.36
$2N^*$ -4p-CMB	(1379, 89)	(1386, 109)	(1613, 42)	(1913, 324)	4.91
$1N_01N^*$ -3p	(1363, 81)	(1377, 128)	—	(1764, 137)	2.51

Here we note that the pole condition (17) depends on both m_1^0 and m_2^0 as can be seen in Eq. (9) for $\tilde{\Sigma}_1(E)$. Thus the mass renormalization of the physical nucleon includes not only the meson cloud effects, but also the contribution from the bare N^* state. If we drop the N^* state, the nucleon pole condition become the usual form

$$m_N = m_1^0 + \Sigma_{11}(m_N). \quad (25)$$

We use the exact conditions (17) and (21) in our investigations. Our approach is not completely consistent with the rigorous approach of Ref. [20], but is sufficient for our present limited purpose of investigating model dependence of resonance extractions. Qualitatively, this model contains the main feature of the coupled-channels model developed in Ref. [12] in handling the πN scattering in P_{11} partial wave. The main difference is in the derivation of meson-baryon potential $v_{MB,M'B'}$ from phenomenological Lagrangians, as discussed in Ref. [19].

III. RESULT

We first discuss the parameters of the coupled-channels models described in section II, which are varied in performing χ^2 fits to empirical P_{11} amplitudes using MINUIT. The non-resonant amplitude $t_{MB,M'B'}$ of Eq. (1) is determined by the coupling constants and cutoffs of form factors of the meson-exchange interactions $v_{MB,M'B'}$ through solving the coupled-channels integral equation (2). In the JLMS fit [17] to the πN data, these parameters were constrained within the ranges known from previous studies of meson-exchange mechanisms, as discussed in Ref. [16]. Here we allow them to vary much more freely such that several models are obtained for examining whether the resulting pole positions are stable against the variation of the analytic properties of the resulting amplitudes.

In the absence of theoretical input, our main challenge is to determine the bare N^* mass $m_{N^*}^0$ and the $N^* \rightarrow MB$ vertex function. For P_{11} partial wave, the number of N^* parameters is: $N_{N^*} + N_{N^*} \times \sum_{MB} n_{v,MB}$, where N_{N^*} is the number of the bare N^* and $n_{v,MB}$ is the number of parameters needed to parameterize each $N^* \rightarrow MB$ vertex function $\Gamma_{N^* \rightarrow MB}$. In our fit

we have $N_{N^*} = 1$ or 2 , and $n_{v,MB} = 2$ ($MB = \pi N, \eta N, \pi \Delta, \sigma N$) or 4 ($MB = \rho N$) from the coupling constants g_{MB} and cutoffs Λ_{MB} (as explained in Ref. [17]). We have total five channels ($N_{MB} = 5$). We thus face a many-parameters problem in fitting the data, which is also present in using the CMB models with $N_{MB} = 8, 6, 3$ in Refs. [3], [10], [9], respectively. We also note that the similar many-parameters problem is also a concern in all approaches of resonance extraction which require high precision fits of πN data. This common problem poses difficulties in assigning the errors for the determined model parameters. We thus follow all previous works and will only assign errors in the determined P_{11} resonance pole parameters which are determined non-linearly by the model parameters associated with meson-exchange interactions $v_{MB,M'B'}$ and bare N^* states.

Our fitting procedure is as follows. We first adjust the parameters associated with the meson-exchange interaction $v_{MB,M'B'}$ to fit P_{11} amplitude at low energies $W \lesssim 1.2$ GeV. To control the number of parameters associated with bare N^* states, we then include only one bare N^* state and try to fit the data in the entire considered energy region by adjusting its bare mass $m_{N^*}^0$ and vertex function parameters g_{MB} and Λ_{MB} . If this fails, we then also allow the parameters associated $v_{MB,M'B'}$ to vary. If this fails again, we then include one more bare N^* state and repeat the process. In the region below $W = 2$ GeV, we find that the considered P_{11} amplitudes can be fitted with one or two bare N^* states. Most of the resulting cutoff parameters are in the range of [500 MeV - 1500 MeV], which are similar to those in typical meson exchange models [18, 20–22, 25]. The bare N^* masses are searched within the range $m_{N^*}^0 \leq 2500$ MeV. The interpretations of these resulting bare N^* parameters with hadron structure calculations remain to be developed. At the present time, they should be considered purely phenomenologically and only the extracted resonance pole parameters have well defined physical meaning.

Once a fit is obtained, we then apply the method of analytic continuation of Ref. [24] to find resonance poles, as also briefly described at the end of Sec. II A. The errors of the resonance parameters are then estimated by using all values obtained in all fits we have performed.

For each of fits to be presented below, we assess its quality by evaluating its χ^2 per data point defined by

$$\chi_{pd}^2 = \sum_{i=1, N_W} \frac{1}{N_{\text{data}}} \left\{ \frac{|\text{Re}[T^{\text{model}}(W_i)] - \text{Re}[T^{\text{data}}(W_i)]|^2}{|\text{Re}(\delta[T^{\text{data}}(W_i)])|^2} + \frac{|\text{Im}[T^{\text{model}}(W_i)] - \text{Im}[T^{\text{data}}(W_i)]|^2}{|\text{Im}(\delta[T^{\text{data}}(W_i)])|^2} \right\} \quad (26)$$

where $T^{\text{data}}(W_i)$ and $\delta[T^{\text{data}}(W_i)]$ are the values and errors of the considered data, respectively; N_W is the number of the energy points where the data exist; $N_{\text{data}} = 2N_W$ is the number of the data points (note that there are real and imaginary components at each energy point). We use the single energy solution SAID-SES as data in our fits, except in one fit using CMB data (see below). As a reference we take the energy dependent solution SAID-EDS as $T^{\text{model}}(E)$ to get $\chi_{pd}^2 = 2.94$, as listed in the first row of Table I along with their values of P_{11} resonance pole positions. Note that their sheet assignments are different from ours since they do not have σN channel. Also they do not have a pole at higher energy region.

We now proceed to present our results by first recalling the three P_{11} poles extracted [14] from using the JLMS parameters. They are listed in the second row of Table I and the corresponding amplitudes (solid curves) are compared with the SAID-EDS [5] (open circles)

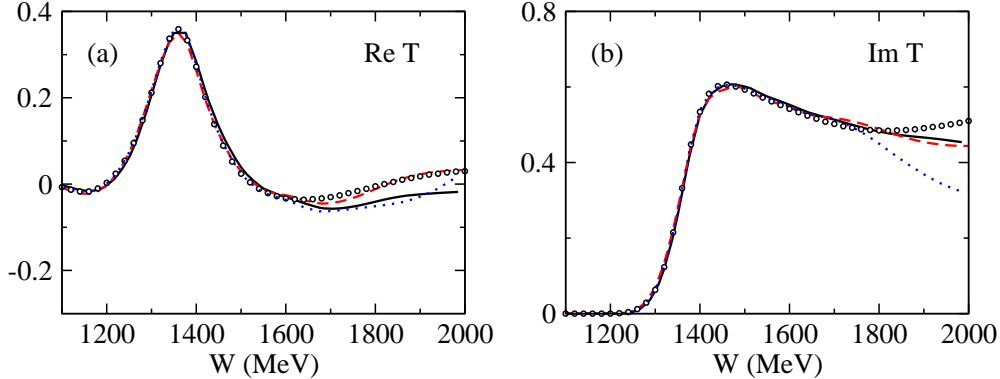


FIG. 1: (Color online) The real (left) and imaginary (right) parts of the on-shell P_{11} amplitudes as a function of the πN invariant mass W (MeV). The solid curves are from the JLMS fit; the dashed (dotted) curves are from the $1N^*-3p-H$ ($1N^*-3p-L$) fit to the SAID-EDS [5] up to $W = 2$ GeV ($W = 1.6$ GeV); the open circles are the SAID-EDS [5]. T is unitless in the convention of Ref. [5].

in Fig. 1. Here we note that the χ_{pd}^2 from the JLMS fit listed in Table I is comparable to that of SAID-EDS. In general, we find it is rather difficult to get a fit with $\chi_{pd}^2 \leq 2.5$ within meson-exchange model, mainly because the errors of SAID-SES are very small in $W \leq 1.45$ GeV region within which the reproduction of the rapid sign changes of empirical amplitude is rather difficult due to the need of delicate balance between the attractive and repulsive effects in different energy region.

In the following subsections, we present results from various fits by varying the dynamical content of the EBAC-DCC model as described above and using a model with a bare nucleon described in Sec. II B.

A. $1N^*-3p-H$ and $1N^*-3p-L$ fits

We first consider the simplest variation of the JLMS fit by including only one bare N^* state, instead of two, to fit the SAID-SES solution. In these fits, the parameters of meson-baryon interactions $v_{MB,M'B'}$ of Eq. (2) are taken from JLMS. We also examine how the extracted resonance poles depend on the data included in the fits. Here we present results from two fits. The solution $1N^*-3p-H$ fits the SAID-SES up to 2 GeV, while the $1N^*-3p-L$ to only 1.6 GeV. These two fits are compared with the JLMS results in Fig. 1. The resulting resonance poles are listed in the third and fourth rows of Table I. We see that the first two poles near the $\pi\Delta$ threshold (~ 1.3 GeV) are in good agreement with those from JLMS. This suggests that these two poles are only sensitive to the data below about 1.5 GeV. The differences between these two fits and JLMS at higher $W > 1.5$ GeV mainly affect the positions of their third poles, as seen in Table I.

The results presented here also indicate that with the nonresonant amplitudes of JLMS, only one bare N^* state is sufficient to describe the πN scattering data up to 2 GeV. All of the fits to be presented below are obtained by starting with non-resonant amplitudes which are chosen to be different from that of JLMS by tuning the parameters of $v_{MB,M'B'}$. It turns out that in these fits, using the procedure described above, two bare N^* states are needed

to get comparable χ^2 .

B. $2N^*$ -3p and $2N^*$ -4p fits

Here we investigate the dependence of the extracted resonances on the accuracy of the employed partial-wave amplitudes by considering the SAID-SES solution which show some oscillating structure in the high $W \gtrsim 1.5$ GeV region. Such a structure is absent in the SAID-EDS (open circles in Fig. 1). From the empirical point of view, it raises the question on whether the fits to the smooth SAID-EDS miss some resonance physics of the original πN data. Before more precise empirical amplitudes are available, it is necessary to explore the extent to which these experimental uncertainties can affect the resonance extractions. We explore this issue by allowing the parameters associated with meson-baryon interaction $v_{MB,M'B'}$ to deviate from the JLMS values in varying these parameters along with the bare N^* parameters in minimizing χ_{pd}^2 . In general, the resulting $\pi N\Delta$ and ρNN coupling constants from these new fits are weaker than the JLMS values and hence give rather different non-resonant amplitudes $t_{\pi N, \pi N}$.

We have obtained several fits which differ from each other mainly in how the oscillating structure of the data at high W are fitted. The results from the $2N^*$ -3p (dotted curves) and $2N^*$ -4p (dashed curves) fits are compared with the JLMS fit (solid curves) in Fig. 2. The resulting resonance poles are listed in the 5th and 6th rows of Table I. Here we see again the first two poles near the $\pi\Delta$ threshold from both fits agree well with the JLMS fit. This seems to further support the conjecture that these two poles are mainly sensitive to the data below $W \sim 1.5$ GeV where the SAID-SES has rather small errors. However, the $2N^*$ -4p fit has one more pole at $M_R = 1630 - i45$ MeV. This is perhaps related to its oscillating structure near $W \sim 1.6$ GeV (dashed curves), as shown in the Figs. 2(b) and 2(d). On the other hand, this resonance pole could be fictitious since the fit $2N^*$ -3p (dotted curve) with only three poles are equally acceptable within the fluctuating experimental errors. Our result suggests that it is important to have more accurate data in the high W region for a high precision resonance extraction.

C. $2N^*$ -4p-CMB fit

To further explore the dependence of the resonance poles on the data, we consider a solution from CMB collaboration [3]. This solution differs significantly from the SAID-SES mainly at $W > 1.55$ GeV. For our present purpose of investigating the stability of the lowest two poles near the $\pi\Delta$ threshold, we fit the data which is obtained from replacing SAID-SES in the high $W > 1.55$ GeV region by the CMB solution. The results (dashed curves) from this fit with all parameters allowed to vary within the EBAC-DCC model are compared with that of the $2N^*$ -4p (solid curves) in Fig. 3. We see that both have oscillating behavior near $W \sim 1.6$ GeV and this could be the common reason why both have an addition pole near $W \sim 1.6$ GeV, as seen in rows 6 and 7 of Table I. The large differences in their fits at high W make their poles near $W \sim 1.9$ GeV very different; in particular their imaginary parts. On the other hand, their lowest two poles near the $\pi\Delta$ threshold are close to other fits discussed so far. This again supports the above observation that these two poles are determined only by the data below $W < 1.5$ GeV which are reproduced very well in all fits.

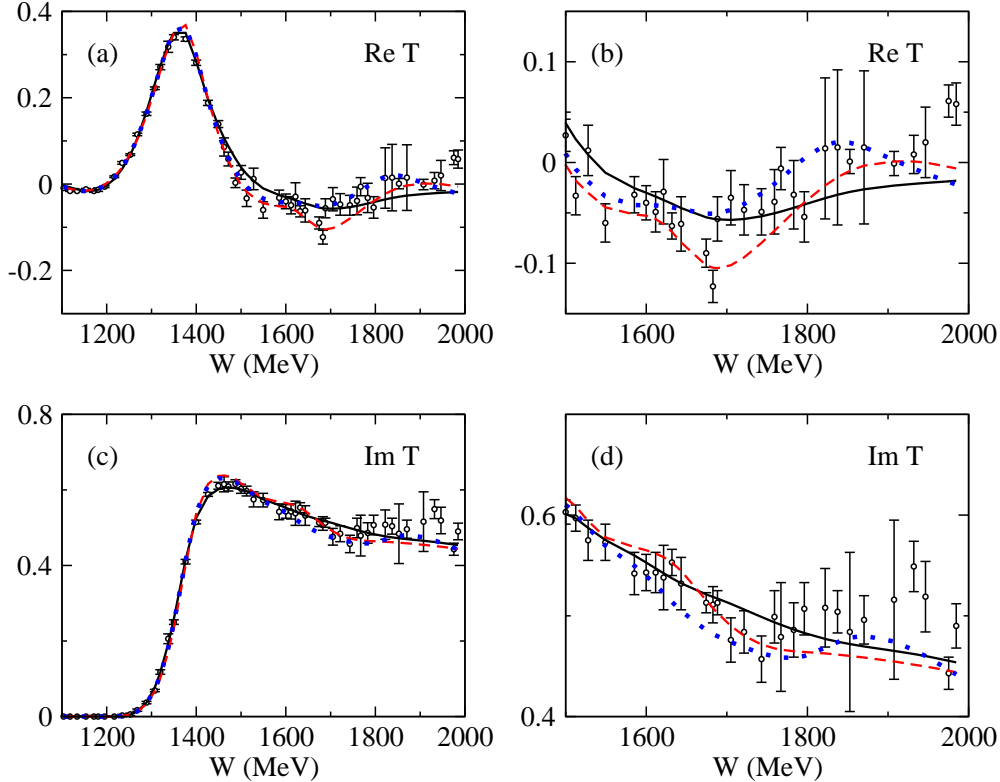


FIG. 2: (Color online) The real (upper panels) and imaginary (lower panels) parts of the P_{11} amplitudes as a function of the πN invariant mass W (MeV). The JLMS (solid) results are compared with the results from the $2N^*-3p$ (dotted) and $2N^*-4p$ (dashed) fits. The points with errors are from the SAID-SES [5]. T is unitless in the convention of Ref. [5].

D. $1N_01N^*-3p$

Here we consider the question concerning whether the analytic structure of the employed reaction model in the $W \leq m_N + m_\pi$ unphysical region can strongly influence the resonance extractions. We first note that most of the resonances listed by Particle Data Group [15] (PDG) are from analysis which treat nucleon as a structureless basic degree of freedom in describing the πN reactions; such models are used in SAID [5] and CMB [3]. Similar simplification is used in formulating the EBAC-DCC model [16]. On the other hand, a more elaborated approach has been taken to analyze πN data using models within which the nucleon is made of a bare nucleon N_0 and meson clouds. Such models [12, 20–22] need to account for the nucleon pole condition, as described in Sec. II B, in fitting the πN reaction data. While all of these models give similar P_{11} amplitudes from threshold $W_{th} = m_N + m_\pi$ to about 1.6 GeV, their analytic structure as function of the complex energy could be very different in the $W \leq m_N + m_\pi$ region where all dynamical models [12, 17, 20–22, 25] have various singularities due to the parameterization of the considered meson-baryon interactions. This is discussed in Ref. [19]. The question is whether such differences can lead to very different resonance poles.

We investigate this issue by comparing the results presented above with that from the fits using the model with a bare N_0 described in Sec. II B. In these fits, the parameters of the

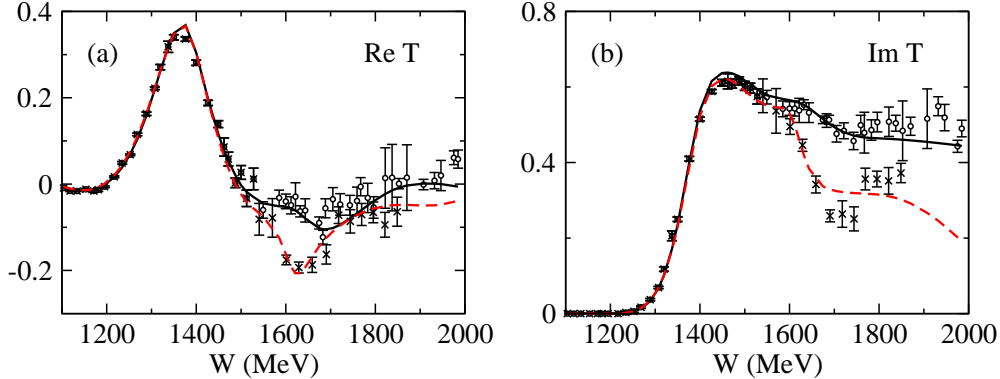


FIG. 3: (Color online) The real (left) and imaginary (right) parts of the P_{11} amplitudes as a function of the πN invariant mass W (MeV). The $2N^*-4p$ fit (solid) and the $2N^*-4p$ -CMB fit (dashed) are compared with the data. The open circles with errors are from the SAID-SES [5], and the crosses with errors are from the SAID-SES at $W < 1.55$ GeV and the CMB solution [3] at $W > 1.55$ GeV. T is unitless in the convention of Ref. [5].

meson-baryon interaction $v_{MB,M'B'}$ are adjusted along with the parameters associated with N_0 and N^* in fitting the SAID-SES up to $W = 2$ GeV under the nucleon pole condition (17) and (21). The results from one of the fits (dashed curves) are compared with the JLMS fits (solid curves) in Fig. 4. We see that the two fits agree very well below $W = 1.5$ GeV, while their differences are significant in the high W region, as seen in the right-hand-side panels of Fig. 4. The resulting resonance poles are given in the last row of Table I. Similar to all of the cases discussed above, we also see here that the first two poles near the $\pi\Delta$ threshold are close to those of JLMS. Our results seem to indicate that these two poles are rather insensitive to the analytic structure of the amplitude in the region below πN threshold, and are mainly determined by the data in the region $m_N + m_\pi \leq W \leq 1.6$ GeV. The third pole from this fit is close to that of JLMS, except that its imaginary part is smaller as seen in the first and last rows of Table I.

E. Averaged values of the extracted P_{11} resonances

To get the averaged values of the extracted P_{11} resonance poles, we take the values listed in Table I except those from models $1N^*-3p$ -L and $2N^*-4p$ -CMB which are obtained from fitting different sets of data, as described above. We further omit the values from $2N^*-4p$ in the evaluation since it has one more pole due to its oscillating behavior (dashed curves in Fig.2) which needs further investigations although it is within the experimental uncertainties. Our values are listed in Table II. The errors are assigned by the differences between the largest and smallest values listed in Table I.

The model parameters from our fits are not relevant to the discussions given above and are therefore not presented. These information is available upon requests.

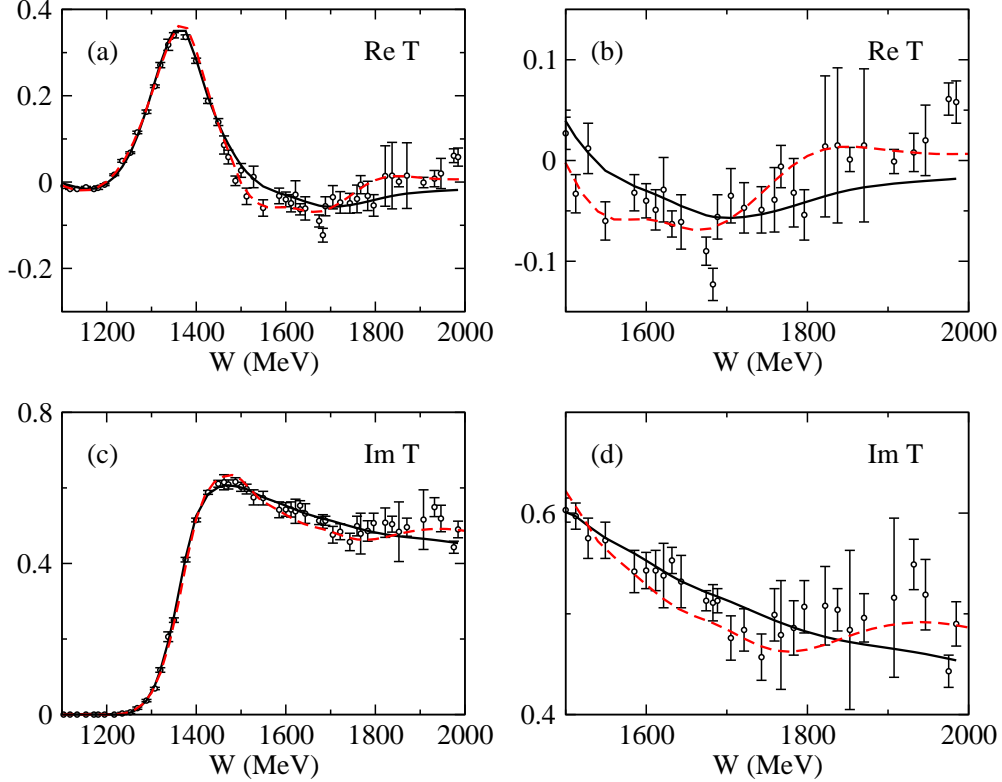


FIG. 4: (Color online) The real (upper panels) and imaginary (lower panels) parts of the P_{11} amplitudes as a function of the πN invariant mass W (MeV). The JLMS fit (solid) and the $1N_01N^*-3p$ fit (dashed) are compared with the SAID-SES [5]. T is unitless in the convention of Ref. [5].

TABLE II: Averaged values of the extracted P_{11} resonances [listed as $(\text{Re}M_R, -\text{Im}M_R)$ in the unit of MeV]. Here we identify these poles with the states listed by PDG [15]. The location of the pole is specified by, e.g., $(s_{\pi N}, s_{\eta N}, s_{\pi\pi N}, s_{\pi\Delta}, s_{\rho N}, s_{\sigma N}) = (upuupp)$, where p and u denote the physical and unphysical sheets for a given reaction channel, respectively.

States	Location	Averaged values (MeV)
$N(1440)$	$(upuupp)$	$(1363_{-6}^{+9}, 79_{-5}^{+3})$
	$(upuppp)$	$(1373_{-10}^{+12}, 114_{-9}^{+14})$
$N(1710)$	$(uuuuup)$	$(1829_{-65}^{+131}, 192_{-110}^{+88})$

IV. SUMMARY AND DISCUSSIONS

In this work we have investigated the extraction of P_{11} nucleon resonances. By performing extensive fits to SAID-SES, we show that two resonance poles near the $\pi\Delta$ threshold are stable against large variations of parameters of meson-exchange mechanisms within EBAC-DCC model [16]. This two-pole structure is also obtained in an analysis based on a model with a bare nucleon state. Our results indicate that the extraction of P_{11} resonances is insensitive to the analytic structure of the amplitude in the region below πN threshold.

By performing different fits to the structure of SAID-SES as well as the old, perhaps also outdated, CMB data, we demonstrated that the number of poles in the $1.5 \text{ GeV} \leq W \leq 2 \text{ GeV}$ region could be more than one. Thus our determination of the resonance poles in this higher W region is not so conclusive. We can only report one pole near $N(1710)$ state listed by PDG, in agreement with several previous analyses. Our results indicate the need of more accurate πN reaction data in the $W > 1.5 \text{ GeV}$ region for high precision resonance extractions. In particular, accurate inelastic amplitudes for ηN , $\pi\Delta$, ρN , and σN channels are highly desirable for our 5-channels analysis. This will allow simultaneous fits to both elastic and inelastic amplitudes to firmly determine the nucleon resonances in the $1.5 \text{ GeV} \leq W \leq 2 \text{ GeV}$ region. The importance of performing multi-channel fits was demonstrated in a recent 3-channels CMB analysis [9] in which it was shown that a simultaneous fit to both $\pi N \rightarrow \pi N$ and $\pi N \rightarrow \eta N$ is needed to establish $N(1710)$ state. Thus it is important to obtain more extensive data of πN reactions including polarization observables such that high precision partial-wave amplitude analysis of $\pi N \rightarrow \pi\pi N$ data can be performed. Such experiments are possible in new hadron facility J-PARC in Japan.

Finally, we like to mention that the analysis of electromagnetic π and 2π production data can help confirm the nucleon resonances extracted from πN reaction data, although its main objective is to extract electromagnetic properties of nucleon resonances. On the other hand, some resonances, which have small branching ratios to π and 2π channels and have large ones for KY and ωN channels, could be identified from analyzing the data of $\gamma N \rightarrow KY, \omega N$ which have been accumulated extensively in recent years. This is also an important task in N^* study before the hadronic data for these channels become extensive at new hadron facility.

Acknowledgments

This work is supported by the U.S. Department of Energy, Office of Nuclear Physics Division, under Contract No. DE-AC02-06CH11357, and Contract No. DE-AC05-06OR23177 under which Jefferson Science Associates operates Jefferson Lab, and by the Japan Society for the Promotion of Science, Grant-in-Aid for Scientific Research(C) 20540270. This research used resources of the National Energy Research Scientific Computing Center, which is supported by the Office of Science of the U.S. Department of Energy under Contract No. DE-AC02-05CH11231.

-
- [1] V. Burkert and T.-S. H. Lee, *Int. J. Mod. Phys. E* **13**, 1035 (2004).
 - [2] R. E. Cutkosky, C. P. Forsyth, R. E. Hendrick, and R. L. Kelly, *Phys. Rev. D* **20**, 2839 (1979)
 - [3] R. E. Cutkosky and S. Wang, *Phys. Rev. D* **42**, 235 (1990).
 - [4] R. A. Arndt, J. M. Ford, and L. D. Roper, *Phys. Rev. D* **32**, 1085 (1985).
 - [5] R. A. Arndt, W. J. Briscoe, I. I. Strakovsky, and R. L. Workman, *Phys. Rev. C* **74**, 045205 (2006) (other references therein).
 - [6] G. Höhler, *Pion-nucleon scattering* (Springer-Verlag, Berlin 1983), Vol. I/92.
 - [7] D. M. Manley, E. M. Saleski, *Phys. Rev. D* **45**, 4002 (1992).
 - [8] M. Batinic, I. Slaus, A. Svarc, and B. M. K. Nefkens, *Phys. Rev. C* **51**, 2310 (1995); M. Batinic, I. Dadić, I. Slaus, A. Svarc, B. M. K. Nefkens, and T.-S. H. Lee, *Phys. Scr.* **58**, 15 (1998).

- [9] S. Ceci, A. Svarc, B. Zauner, Phys. Rev. Lett. **97**, 062002 (2006).
- [10] T. P. Vrana, S. A. Dytman, T.-S. H. Lee, Phys. Rept. **328**, 181 (2000).
- [11] G. Y. Chen, S. S. Kamalov, S. N. Yang, D. Drechsel, L. Tiator, Phys. Rev. C **76**, 035206 (2007).
- [12] M. Döring, C. Hanhart, F. Huang, S. Krewald, and U.-G. Meißner, Nucl. Phys. **A829**, 170 (2009).
- [13] A. V. Sarantsev *et al.* (CB-ELSA and A2-TAPS Collaborations), Phys. Lett. **B659**, 94 (2008)
- [14] N. Suzuki, B. Juliá-Díaz, H. Kamano, T.-S. H. Lee, A. Matsuyama, and T. Sato, Phys. Rev. Lett. **104**, 042302 (2010).
- [15] C. Amsler *et al.* (Particle Data Group), Phys. Lett. **B667**, 1 (2008).
- [16] A. Matsuyama, T. Sato, and T.-S. H. Lee, Phys. Rep. **439**, 193 (2007).
- [17] B. Juliá-Díaz, T.-S. H. Lee, A. Matsuyama, and T. Sato, Phys. Rev. C **76**, 065201 (2007).
- [18] A. M. Gasparyan, J. Haidenbauer, C. Hanhart, and J. Speth, Phys. Rev. C **68**, 045207 (2003).
- [19] B. Juliá-Díaz, H. Kamano, T.-S. H. Lee, A. Matsuyama, T. Sato, and N. Suzuki, Chin. J. Phys. **47**, 142 (2009); arXiv:0902.3200 [nucl-th].
- [20] B. C. Pearce and I. R. Afnan, Phys. Rev. C **34**, 991 (1986); **40**, 220 (1989).
- [21] F. Gross and Y. Surya, Phys. Rev. C **47**, 703 (1993).
- [22] C. T. Hung, S. N. Yang, and T.-S. H. Lee, Phys. Rev. C **64**, 034309 (2001).
- [23] See, for example, A. Klein and T.-S. H. Lee, Phys. Rev. D **10**, 4308 (1974)
- [24] N. Suzuki, T. Sato, and T.-S. H. Lee, Phys. Rev. C **79**, 025205 (2009); arXiv:1006.2196[nucl-th].
- [25] T. Sato, T.-S. H. Lee, Phys. Rev. C **54**, 2660 (1996).